Journal of Information & Communication Technology
Vol. 9, No. 1, (Spring2015) 01-12

Local Binary Signed Pressure Force Function Based Variation Segmentation Model.

Tariq Ali *
Institute of Social Policy & Research (ISPAR), Peshawar, Pakistan.

Lutful Mabood *
Department of Mathemetics, University of Peshawar.

Haider Ali *
Department of Mathemetics, University of Peshawar.

Noor Badshah *
Department of Basic sciences, UET Peshawar.

ABSTRACT

Global and local image information is crucial for accurate segmentation of images with intensity inhomogeneity, valuable minute details and multiple objects with various intensities. However, local information is not embedded in popular region-based active contour models, such as the Sign Pressure force (Spf) function based active contour model by K. Zhang et al. In this paper, we propose a region-based active contour model which is able to utilize together image information in local regions and global information. The major contribution of this paper is the introduction of a new local signed pressure force function, which enables the extraction of accurate local and global image information. Therefore, our model can be used to segment images with intensity inhomogeneity, minute valuable details and multiple objects with several intensities. Comparison tests show the advantages of our method in terms of robustness.

Keywords : Image segmentation, Level set method, Signed pressure force function, Local binary fitting terms.

---

*The material presented by the authors does not necessarily portray the viewpoint of the editors and the management of the Institute of Business and Technology (IBT) or Karachi Institute of Power Engineering.

[1] Tariq Ali : shariq.tk57@gmail.com
[2] Lutful Mabood : lathizm@gmail.com
[3] Haider Ali : haider_uop99@yahoo.com
[4] Noor Badshah : noor2knoor@gmail.com

1. INTRODUCTION

Image segmentation aims to divide an image in to different region such that each region is similar with respect to color, intensity or texture etc., to find out some useful details from it. In simple words it aims to extract meaningful lying objects in images, either by dividing images into contiguous semantic regions, or by extracting one or several objects more specific in images, such as medical structures. In image segmentation our goal is to distinguish objects from background (J. Lie, M. Lysaker et.al, 2006).

In variation frame work two approaches emerged, namely, edge based and region based techniques. For edge detection most of the models use an edge detector function which mainly depends on the gradient of a given image (D. Terzopoulos ,1988). On the other hand, region based segmentation models are usually found to use region detectors, named as fidelity terms, which use image statistical information to capture objects/regions(W. Zhou et.al, 2010). Both of these methods have some merits and demerits i.e. edge based models utilize only local information which makes it unfits in noisy images. In contrast, region based models utilize only global information as a consequence its results are not promising in images where there is in homogeneity. There are also some models which utilize both edge and region information (K. Chen, 2010). It has also some pros and cons. However, it has been observed from test results that image global and local image information is crucial for accurate segmentation of images with intensity in homogeneity, valuable minute details and multiple objects with various intensities. However global information is not embedded in popular region-based active contour models, such as the Spf function based active contour model by K. Zhang et al.

In this paper, we propose a region-based active contour model which is able to utilize together image information in local and global regions. The major contribution of this paper is the introduction of a new local signed pressure force function, which enables the extraction of accurate local and global image information. Therefore, our model can be used to segment images with intensity in homogeneity, minute valuable details and multiple objects with several intensities. Comparison tests show the advantages of our method in terms of robustness.

2. PREVIOUS WORKS

2.1 The Chan-Vese Model (CV)

Chan and Vese proposed an active contour model which can be considered as a special case of the Mumford-Shah model (J. Shah, 1989). For a given image u(x,y) in domain ?, the CV model proposed to minimize the following energy functional:

$$F^{cv} = \lambda_1 \int_{inside(\Gamma)} |u - c_1|^2 \, dx + \lambda_2 \int_{outside(\Gamma)} |u - c_2|^2 \, dx, \quad (\mathbf{1})$$

Wherec_1 and c_2 are two constants which are the average intensities inside and outside the contour ? respectively. With the level set method, we assume

$$\begin{cases} \Gamma = \{(x,y) \in \Omega : \phi(x,y) = 0\}, \\ inside(\Gamma) = \{(x,y) \in \Omega : \phi(x,y) > 0\}, \\ outside(\Gamma) = \{(x,y) \in \Omega : \phi(x,y) < 0\}. \end{cases} \quad (2)$$

By minimizing equation (1), we solve for c_1 and c_2 as follows:

$$c_1 = \frac{\int_\Omega uH(\phi)dxdy}{\int_\Omega H(\phi)dxdy},\ c_1 = \frac{\int_\Omega u(1-H(\phi))dxdy}{\int_\Omega (1-H(\phi))dxdy}. \quad (3)$$

By incorporating the length energy term into equation (1), minimization leads to the following evolution equation

$$\frac{\partial \phi}{\partial t} = \delta(\phi)\left[\mu\nabla.\left(\frac{\nabla\phi}{|\nabla\phi|}\right) - \lambda_1(u-c_1)^2 + \lambda_2(u-c_2)^2\right], \quad (4)$$

Where μ are fixed parameters, μ controls the smoothness of zero level set and control the image data driven force inside and outside the contour respectively. H(Ø)is the Heaviside function and d(Ø) is the dirac delta function. Usually, the following regularized Heaviside and delta is used:

$$H_\varepsilon(z) = \frac{1}{2}\left(1 + \frac{2}{\pi}\arctan\left(\frac{z}{\varepsilon}\right)\right),\ \delta_\varepsilon(z) = \frac{\varepsilon}{\pi(\varepsilon^2 + z^2)}. \quad (5)$$

This model works well whenever intensities are homogeneous inside and outside G. In this case c_1 and c_2are good approximation of uinside and outside G respectively. However, in case of inhomogeneity c_1 and c_2 can be far different from the original data which often effect the quality of the desired result. In order to overcome the weakness of the CV model the LBF model was introduced.

2.2 Local Binary Fitting (LBF) Model

Li et al. (Z. Ding et.al, 2007) proposed the following energy functional:

$$E(\Gamma, f_1, f_2) = \int_\Omega \varepsilon_x^{LBF}(\Gamma, f_1(x), f_2(x))dx. \quad (6)$$

Wheree_x^LBF is defining as:

$$\varepsilon_x^{LBF} = \lambda_1\int_{in(\Gamma)} K(x-y)|u(y) - f_1(x)|^2\,dy + \lambda_2\int_{out(\Gamma)} K(x-y)|u(y) - f_2(x)|^2\,dy \quad (7)$$

Thus the overall energy functional is given by:

$$E(\Gamma, f_1, f_2) = \lambda_1\int_\Omega [\int_{in(\Gamma)} K(x-y)|u(y) - f_1(x)|^2\,dy]dx$$

$$+\lambda_2\int_\Omega [\int_{out(\Gamma)} K(x-y)|u(y) - f_2(x)|^2\,dy]dx, \quad (8)$$

Where 1 and 2 are any two positive numbers, K_s is a Gaussian kernel with standard deviations. In level set formulation the above equation can be written as:

$$E(\Gamma, f_1, f_2) = \lambda_1 \int_\Omega [\int_{in(\Gamma)} K(x-y)|u(y)-f_1(x)|^2 H(\phi(y))dy]dx$$

$$+\lambda_2 \int_\Omega [\int_{out(\Gamma)} K(x-y)|u(y)-f_2(x)|^2 (1-H(\phi(y)))dy]dx. \textbf{(9)}$$

Minimizing with respect to f_1 (x) and f_2 (x) we get:

$$f_1(x) = \frac{K_\sigma * [H_\varepsilon(\phi)u(x)]}{K_\sigma * [H_\varepsilon(\phi)]},\ f_2(x) = \frac{K_\sigma * [(1-H_\varepsilon(\phi))u(x)]}{K_\sigma * [(1-H_\varepsilon(\phi))]}. \textbf{(10)}$$

Now keeping f_1 (x) and f_2 (x) fixed, and minimizing the energy function with respect to Øwe get:

$$\frac{\partial \phi}{\partial t} = -\delta_\varepsilon(\phi)\left(\lambda_1 e_1 - \lambda_2 e_2 + v\delta_\varepsilon(\phi) div\left(\frac{\nabla\phi}{|\nabla\phi|}\right) + \mu\left(\nabla^2\phi - div\left(\frac{\nabla^2\phi}{|\nabla\phi|}\right)\right)\right), \textbf{(11)}$$

Where d_e is the smooth Dirac function, and e_1 and e_2 are the functions define as follow;

$$e_1(x) = \int_\Omega K_\sigma(y-x)|u(x)-f_1(y)|^2 dy$$

$$e_2(x) = \int_\Omega K_\sigma(y-x)|u(x)-f_2(y)|^2 dy.$$

This model performs better than the CV model in segmenting images having in homogeneity.

Another attempt to improve the performance of the CV model is done by the by introducing signed pressure force (Spf) function (Zhang et al., 2010).

2.3 The SBGFRLS Model (CVB)

The CVB model [17, 18] is another attempt in variation modeling to have better segmentation results than GAC and CV model. Based on the concept of Spf function in the CVB model used the following Spf function (J.L. Prince er.al, 2000):

$$Spf(u(x,y)) = \frac{u(x,y) - \frac{c_1+c_2}{2}}{\max\left|u(x,y) - \frac{c_1+c_1}{2}\right|},\quad (x,y) \in \Omega, \textbf{(14)}$$

Wherec_1, c_2 are averages defined in equation (3). The SPF function takes values in the range (N. Badshah, 2011), having the properties of an edge detector function, as its signs modulate inside and outside of the object, where it is assumed that intensities inside and outside of the object are homogeneous. Next, based on the edge detection property of the Spf function, it is substituted in equation;

$$\frac{\partial \phi}{\partial t} = g(|\nabla u|)\left(div\left(\frac{\nabla\phi}{|\nabla\phi|}\right) + \alpha\right)|\nabla\phi| + \nabla g.\nabla\phi, \textbf{(15)}$$

Wherea|?Ø| is the balloon force, which controls the contour shrinking or expanding? Thus we obtain the following evolution equation:

$$\frac{\partial \phi}{\partial t} = Spf\left(div\left(\frac{\nabla \phi}{|\nabla \phi|} \right) + \alpha \right)|\nabla \phi| + \nabla Spf . \nabla \phi . \textbf{(16)}$$

Then, the equation (16) is reduced to the following evolution equation (W. Zhou et.al, 2010):

$$\frac{\partial \phi}{\partial t} = \alpha Spf\,|\nabla \phi|. \textbf{(17)}$$

This model works in simple tests as well as its design is capable to capture the objects of interest. But since it utilizes the global image intensities inside and outside the contour, it has the similar drawbacks to the CV model, such as the inefficiency in handling images with severe intensity in homogeneity (W. Zhou et.al, 2010).

To handle intensity in homogeneity, we introduce a new signed pressure force function which is embedded with both local and global image details.

3. THE PROPOSED MODEL (LBSPF)

We propose the following LbSpf function which use image local and global details proportionally:

$$LbSpf\left(u(x,y)\right) = \frac{u(x,y) - \frac{\left[\lambda(c_1 + c_2) + f_1 + f_2\right]}{2 + 2\lambda}}{\max\left|u(x,y) - \frac{\left[\lambda(c_1 + c_2) + f_1 + f_2\right]}{2 + 2\lambda}\right|}, \quad (x,y) \in \Omega, \textbf{(18)}$$

Where is the weighting parameter? Now it is clear from equation (18) that for inhomogeneous images we have to keep the value of ? small so that the influence of local term is higher than the global information c_1 and c_2,while on the other hand for noisy images we keep the value of ?near to one so that global information can also contribute. Now we plug our proposed LbSpf function in equation (15) thus we obtain:

$$\frac{\partial \phi}{\partial t} = LbSpf\left(div\left(\frac{\nabla \phi}{|\nabla \phi|} \right) + \alpha \right)|\nabla \phi| + \nabla LbSpf . \nabla \phi . \textbf{(19)}$$

Then, the equation (19) is reduced to the following evolution equation (W. Zhou et.al, 2010):

$$\frac{\partial \phi}{\partial t} = \alpha LbSpf\,|\nabla \phi|. \textbf{(20)}$$

Further details about the implementation of our method can be seen in (W. Zhou et.al, 2010).

4. EXPERIMENTAL RESULTS

This section contains some tests results of our proposed LbSpf function along with the test results of well-known CVB model (W. Zhou et.al, 2010). These tests will explicitly reveal that our new model is very efficient in contrast with the compared model in capturing objects in a range of images including medical inhomogeneous images. In all the experiments the first row shows the results of CVB model while second row exhibits the results of our proposed LbSpf function. The first, second, third and fourth columns show initial contour, final contour, segmented result and its corresponding 3D plot respectively. For all experiments the initial contour kept same unless it is specified. Figure 1 shows a real plane image in which both the models work very well as clear from figures 1(c) and 1(g). Figure 2 is a synthetic image with different intensities objects it is clear from 2(c) that CVB model fails to capture all objects, while on the other hand 2(g) shows the successful segmented results of LbSpf. Figure 3 is MR brain image with intensity in homogeneity in which CVB model ignored many details of the image as shown in figure 3(c). In contrast figure 3(g) refers the successful results of LbSpf and it capture all the objects in it. Figure 4 is a medical heart image having intensity in homogeneity with many objects in which CVB model is unable to work efficiently as clear from figure 4(c), while the promising results of LbSpf is clear from figure 4(g). Figure 5 is a MR brain image in which the initial contour kept same and it is clear from figure 5(c) that CVB model only detect the outer layer of the image and even the contour did not inter into image, while on the other hand LbSpf not only detect outer layer but it also capture minute details inside the image as clear from 5(g). Figures 6, 7 and 8 are veins, head and synthetic inhomogeneous images respectively. From figures 6(c), 7(c) and 8(c) it can be seen easily that CVB model is not more able to work in it. In contrast, the results of LbSpf are quite good and it completed the task as clear from figures 6(g), 7(g) and 8(g).

CONCLUSIONS

We have proposed a new LbSpf function for segmenting a range of images with intensity in homogeneity. The tests results have shown that our new LbSpf function performs robustly in severe in homogeneity. However, there is much left to do in our future work. One direction is to extend our model to multi-phase segmentation models and the other could be its extension to related segmentation problems such as texture segmentation.

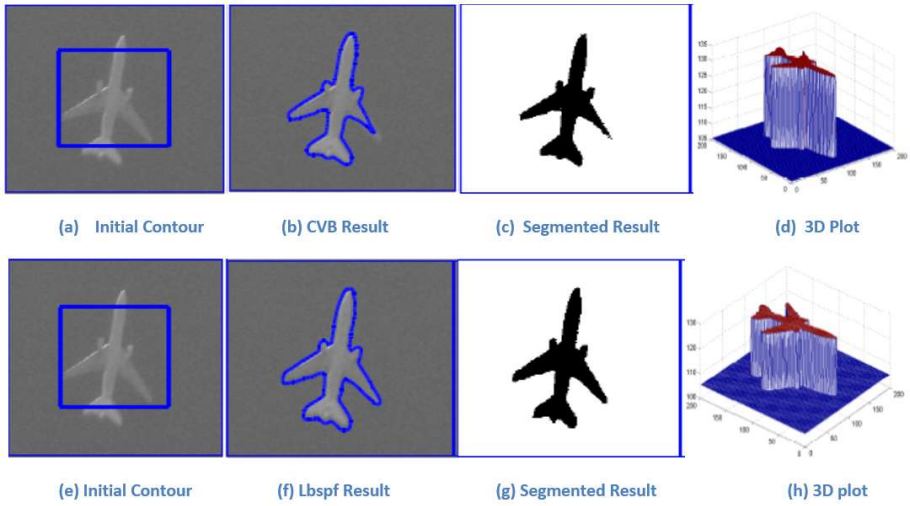

Figure 1: Experimental test exhibiting the performance of the CVB and LbSpf on a real plane image: (Row First) Performance by the CVB model; (Row Second) Performance by the LbSpf model. For the proposed model parameters used are; μ = 10, ? = 1, s = 5, size (u) = 200.

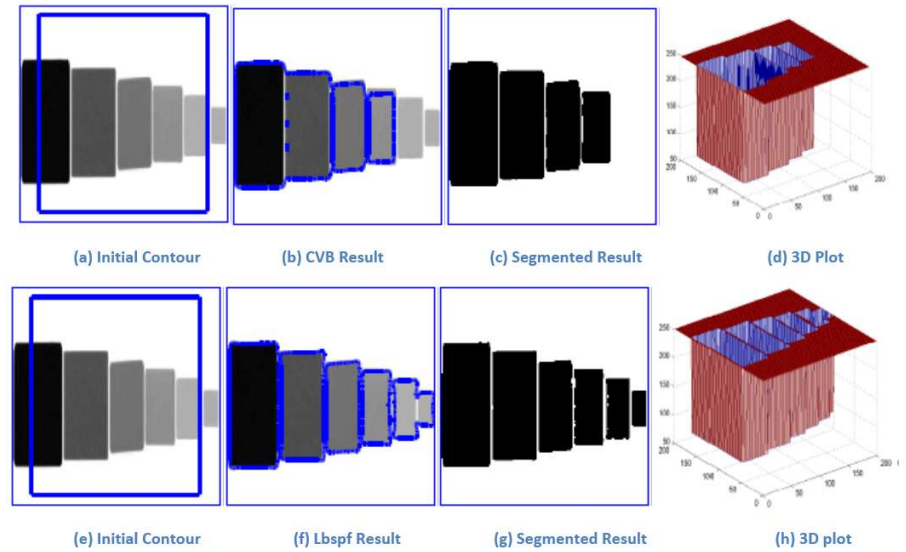

Figure 2: Experimental test displaying the performance of the CVB and LbSpf on a synthetic multi region image: (Row First) Performance by the CVB model; (Row Second) Performance by the LbSpf model. It can be observed that the proposed LbSpf model performed far better than the CVB model. For the proposed model parameters used are; μ = 20, ? = 0.1, s = 3, size(u) = 200 × 200.

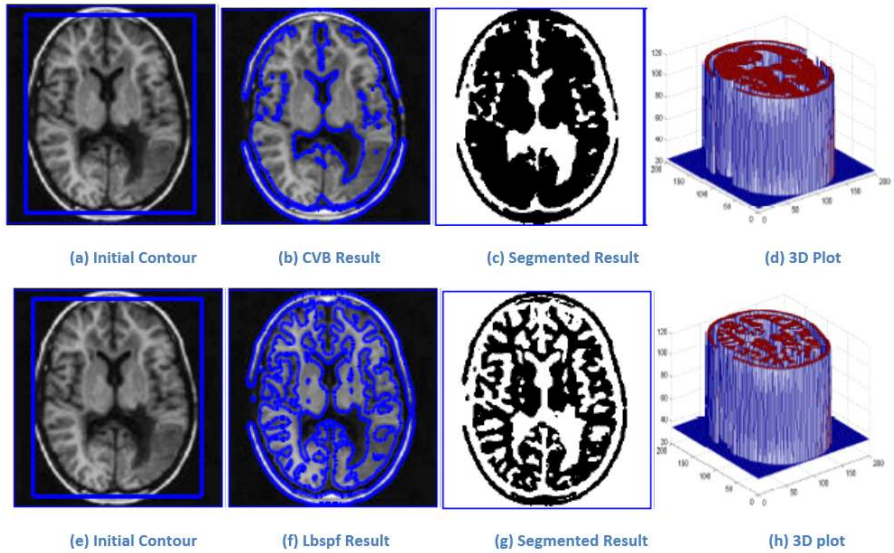

Figure 3: Experimental test showing the performance of the CVB and LbSpf on a real medical brain image: (Row First) Performance by the CVB model; (Row Second) Performance by the LbSpf model. It can be easily observed that the proposed LbSpf model performed far better than the CVB model. For the proposed model parameters used are; μ = 25, ? = 0.1, s = 5, size(u) = 200 × 200.

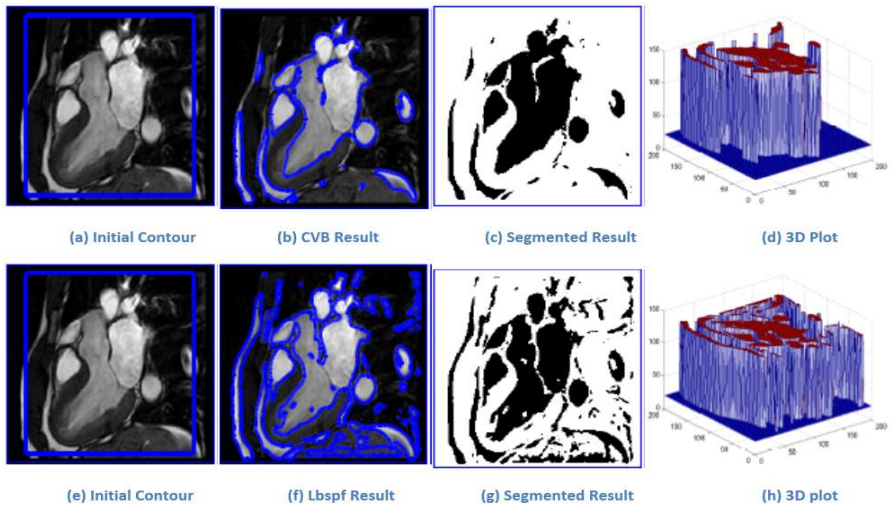

Figure 4: Experimental test exhibiting the performance of the CVB and LbSpf on a real medical cardiac image: (Row First) Performance by the CVB model; (Row Second) Performance by the LbSpf model. It can be easily observed that the proposed LbSpf model performed far better than the CVB model. For the proposed model parameters used are; μ = 29, ? = 0.2, s = 5, size(u) = 200 × 200.

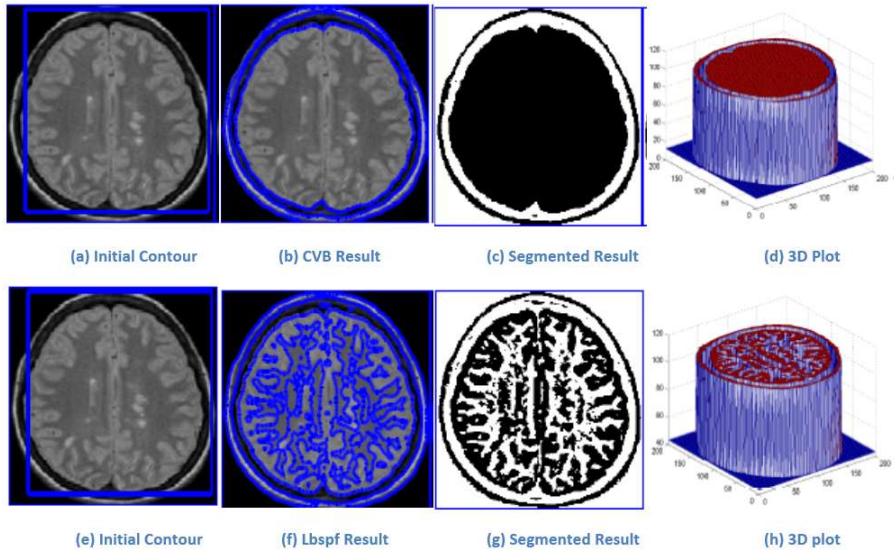

Figure 5: Experimental test displaying the performance of the CVB and LbSpf on a real medical brain image: (Row First) Performance by the CVB model; (Row Second) Performance by the LbSpf model. For the proposed model parameters used are; μ = 35, ? = 0.07, s = 4, size (u) = 200 × 200.

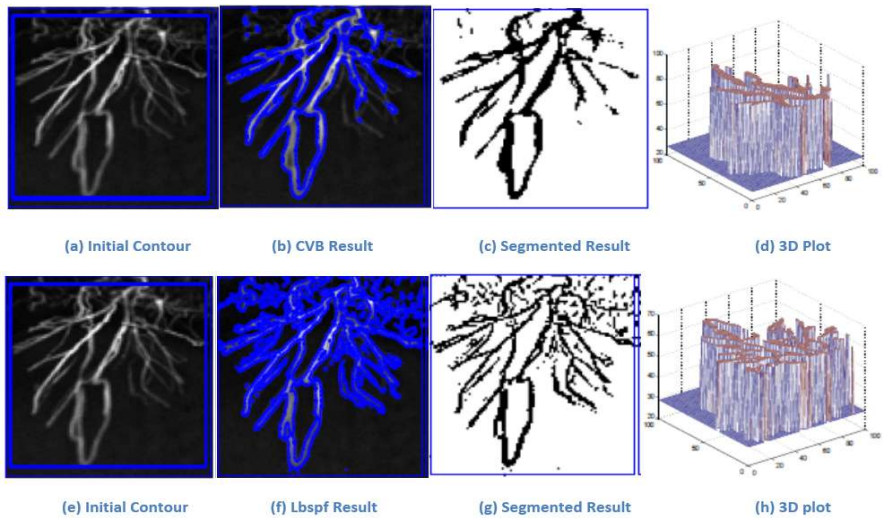

Figure 6: Experimental test showing the performance of the CVB and LbSpf on a real medical vessels image: (Row First) Performance by the CVB model; (Row Second) Performance by the LbSpf model. It can be very easily observed that the proposed LbSpf model performed robustly than the CVB model. For the proposed model parameters used are; μ = 25, ? = 0.01, s = 1, size(u) = 100 × 100.

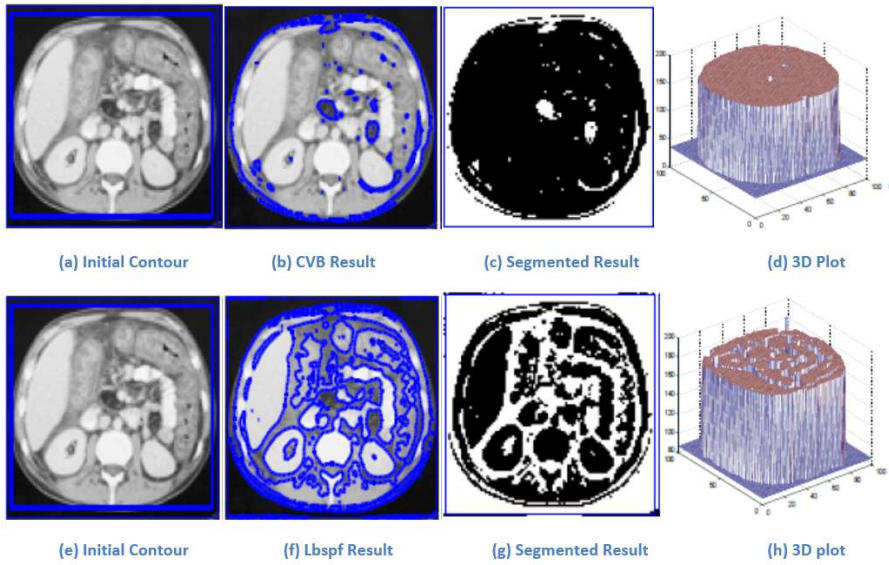

Figure 7: Experimental test exhibiting the performance of the CVB and LbSpf on a real medical abdominal image: (Row First) Performance by the CVB model; (Row Second) Performance by the LbSpf model. It can be very easily observed that the proposed LbSpf model performed robustly than the CVB model. For the proposed model parameters used are; μ = 30, ? = 0.001, s = 1, size(u) = 100 × 100.

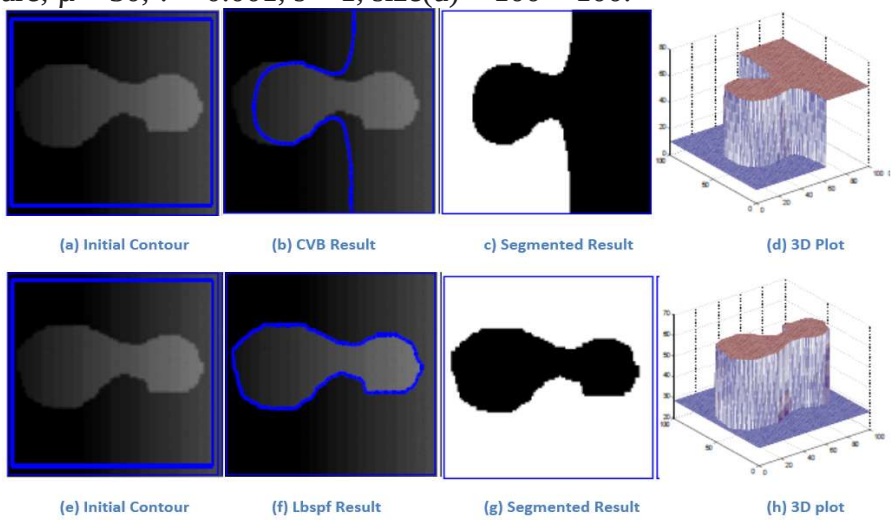

Figure 8: Experimental test exhibiting the performance of the CVB and LbSpf on a real medical abdominal image: (Row First) Performance by the CVB model; (Row Second) Performance by the LbSpf model. It can be very easily observed that the proposed LbSpf model performed robustly than the CVB model. For the proposed model parameters used are; μ = 30, ? = 0.001, s = 1, size(u) = 100 × 100.

ACKNOWLEDGEMENT:

In would like to Special thanks to my co-authors Mr.Tariq Ali, Lutful Mabood, Mr.Haider Ali and Mr. Noor Badshah, Assistance Professor, Faculty of Mathematics and Basic Science, for his leadership, capable supervision of full that played an effervescent part in execution of this work. I emphatically wish to thank Dr. Mansoor Zafar Dawood, The Dean faculty of Computer Science for providing me convenient way of action throughout my research work.

I would like to extend my sincere appreciation and acknowledgment for valuable guidance the selfless cooperation of Institute of Social Policy & Research (ISPAR), Peshawar, Pakistan, University of Peshawar and other libraries.

At the end, I am profoundly grateful to all my family members whose endurance and understanding have played a significant role in my success by sacrificing the important family time and supporting me all over the research work.

REFERENCES

[1] N. Badshah, K. Chen, H. Ali and G. Murtaza. Coefficient of Variation Based Image Selective Segmentation Using Active Contour. East Asian Journal on Applied Mathematics, 2(2): 150–169, May 2012.

[2] N. Badshah and K. Chen. Image Selective Segmentation Under Geometrical Constraints Using an Active Contour Approach. Math. Comp., 7: 759–778, 2010.

[3] V. Caselles, R. Kimmel and G. Sapiro. Geodesic Active Contours. International Journal of Computer Vision, 22(1): 61–79, 1997.

[4] T. F. Chan and L. A.Vese.Active Contours without Edges. IEEE Transactions on Image Processing, 10(2): 266–277, 2001.

[5] C. Gout, C. L. Guyader and L. A. Vese. Segmentation under Geometrical Conditions with Geodesic Active Contour and Interpolation using Level set Method. Numerical Algorithms, 39: 155–173, 2005.

[6] C. L. Guyader and C. Gout. Geodesic active contour under geometrical conditions theory and 3D applications. Numerical Algorithms, 48: 105–133, 2008.

[7] M. Jeon, M. Alexander, W. Pedrycz, and N. Pizzi. Unsupervised hierarchical imagesegmentation with level set and additive operator splitting. PRL., 26(10): 1461–1469, 2005.

[8] M. Kass, A. Witkin and D. Terzopoulos. Active Contours Models. International Journal of Computer Vision, 321–331, 1988.

[9] C.M. Li, C. Kao, J. Gore, Z. Ding, Implicit Active Contours Driven by Local Binary Fitting Energy, in: IEEE Conference on Computer Vision and Pattern Recognition, 2007.

on Pure Applied Mathematics, 42: 577–685, 1989.

[11] G. Murtaza, H. Ali and N. Badshah. A Robust Local Model for Segmentation Basedon Coefficient of Variation. Journal of information & Communication Technology, 5(1): 30–39, 2011.

[12] X. C. Tai and O. Christiansen. Image Segmentation Using Some Piecewise Constant Level Set Methods with MBO Type of Projection. Int. J. Computer Vision, 73(1): 61–76, 2007.

[13] J. Lie, M. Lysaker and X. C. Tai.A Variant of the Level Set Method and Applications to Image Segmentation. Mathematics of Computation,75(255): 1155–1174, 2006.

[14] L. A. Vese and T. F. Chan. A Multiphase Level set Framework for Image Segmentation using the Mumford and Shah Model, Int. J. Computer Vision, 50(3): 271–293, 2002.

[15] X. F. Wang, D. S. Huang, H. Xu. An efficient Local Chan-Vese Model for Image Segmentation. Pattern Recognition , 43: 603–618, 2010.

[16] C.Y. Xu, A. Yezzi Jr., J.L. Prince, On the Relationship between Parametric and Geometric Active Contours, in: Processing of 34thAsilomar Conference on Signals Systems and Computers, 483–489, 2000.

[17] C. Zhang, Y. Zhang, Z. Lin, Automatic Face Segmentation Based on the LevelSet Method. National Conference on Information Technology and Computer Science, 678–681, 2012.

[18] K. Zhang, L. Zhang, H. Song, W. Zhou, Active Contours with Selective Local or Global Segmentation: A new Formulation and Level Set Method. Image and Vision Computing, 28: 668–676, 2010.